

## Luminescence of compacts from mixtures of nano and micro calcium fluoride powders

V. Ilves<sup>1,\*</sup>, S. Sokovnin<sup>1,2</sup>, S. Zayats<sup>1</sup>, M. Zuev<sup>3</sup>

<sup>1</sup>*Institute of Electrophysics UB RAS, Yekaterinburg, Russia*

<sup>2</sup>*Ural Federal University Named after the first President of Russia B.N. Yeltsin, Yekaterinburg, Russia*

<sup>3</sup>*Institute of Solid State Chemistry UB RAS, Yekaterinburg, Russia*

\**ilves@iep.uran.ru*

**Abstract.** There were carried out the studies of pulsed cathodoluminescent (PCL) and photoluminescent (PL) properties of compacts made by static (SP) and magnetic-pulse (MP) pressing from mechanical mixtures of micro and nano calcium fluoride powders. The mixtures contained commercial powder (TU 6-09-2412-84) and nanopowder (NP) CaF<sub>2</sub> (NP produced by pulsed electronic evaporation at the installation NANOBEAM-2 in vacuum) at powder weight ratios: 10:0.125 – 10:1. Was shown the effect of the concentration of the CaF<sub>2</sub> nanoadditive, the pressing temperature ( $T_p$ ) and the preliminary annealing of the nanoadditive on the density of compacts. Presence of nanoparticles (NPles) of Ca at NP, strong defective structure and high porosity of NP had strong impact on luminescent characteristics of the compacts made both of clean NP CaF<sub>2</sub> and from their mixes. Annealing of the initial NP at a temperature of 400 °C made it possible to achieve the same density of compacts of pure micropowders and nanopowders (89% of the theoretical density) using the MPP method with heating. The maximum density of compacts from mixtures of powders of different dispersity did not exceed 78% of the theoretical density. The main factor that influenced the morphology of PCL spectra of all compacts, without exception, was the compaction temperature (425 °C) in the MPP method. The blue peak (434 nm) is associated with an impurity oxygen vacuum in the nanocrystalline CaF<sub>2</sub> lattice and was found in the photoluminescence spectra of compacts from NP annealed at 400 °C. The morphology of the PL spectra is more sensitive to the influence of various factors (concentration of the nanoadditive, pressing method, pressing pressure, etc.) in comparison with the morphology of the PCL spectra. Is given the study of the density and transparency of ceramics from the above compacts after annealing the compacts in vacuum at a temperature of 1000 °C.

**Keywords:** calcium fluoride compacts, pulsed cathodoluminescence, photoluminescence.

### 1. Introduction

In the early 21st century was revived interest in fluoride nanoceramics. Vacuum chambers are required to prevent pyrohydrolysis of fluorides [1]. The choice of precursors is also given special attention. The authors previously used pulsed electron beam evaporation in vacuum (PEBE) [2] to produce nanopowders (NPs) CaF<sub>2</sub> [3], BaF<sub>2</sub> [4] and CeF<sub>3</sub> [5]. Nanoparticles (NPles) of reduced Ca CaF<sub>2</sub> found in the NP. Compaction of metal-fluoride NP is a little studied topic. Advantages of NP fluorides produced by PEBE are the small NPles size (from 3 to 15 nm) and big specific surface area (SSA) of NP. Annealing fluorides at a temperature of 400–450 °C does not significantly increase the grains of nanocrystals [3–5]. Unfortunately, the mesoporous type of NP fluorides (PEBE) is undesirable for the manufacture of optically transparent nanoceramics. However, the porosity of these NPs is interparticular and the NPles are quasi-spherical. Interparticle pores may partially disappear when pressed and recrystallized by sintering the compact in a vacuum or inert gas. The purpose of the work was to study the influence of small additives of NP CaF<sub>2</sub> on the density and luminescent characteristics of compacts from mechanical mixtures of nano and micro CaF<sub>2</sub> powders compressed using static and magnetic pulse pressing and to assess the potential of compacts for applied fields of science and technology.

### 2. Experimental

The following were used in the work: commercial submicron powder of CaF<sub>2</sub> brand OCH (TU 6-09-2412-84) and NP CaF<sub>2</sub> produced by PEBE in vacuum [2]. The powders are mixed in a

porcelain mortar at weight ratios of powders: 10:0.125, 10:0.25, 10:0.5 and 10:1. Compacts are compacted from the mixtures by magnetic pulse pressing (MP) at 425 °C and room temperature (RT) and static pressing (SP) at RT. NP CaF<sub>2</sub> (PEBE) was used as an additive in commercial matrix powder. Diffractograms were recorded on a D8 DISCOVER diffractometer on copper radiation (Cu K $\alpha$ 1,2  $\lambda$  = 1.542 Å). Photoluminescence spectra (PL) were recorded on a MDR-204 spectrometer with a deuterium lamp DDS-30, with a light filter (0.6–1  $\mu$ m) and smoothing out the noisy spectra. Pulsed cathodoluminescence spectra (PCL) are recorded on the RT KLAVI-1 installation.

### 3. Results and discussion

NP CaF<sub>2</sub> contained a cubic and tetragonal fluorite phase, S.G.: Fm-3m (225); PDF Card No. 00-035-0816. Micron powder also consisted of cubic and tetragonal fluorite phases, PDF No. 00-035-0816. The sizes of the coherent scattering regions (CSR) and the lattice periods of the micro and NP phases are given in Table 1.

**Table 1.** Lattice Parameters and CSR in Cubic and Tetragonal Phases of Commercial and Nano CaF<sub>2</sub> Powder

CaF <sub>2</sub> commercial					
CaF <sub>2</sub> cub			CaF <sub>2</sub> tetr		
CSR, nm	Period, Å	$\rho$ , g/cm <sup>3</sup>	CSR, nm	Period, Å	$\rho$ , g/cm <sup>3</sup>
30(2)	5.465(3)	3.177(4)	14(2)	$a = 3.784(7)$ $c = 2.604(6)$	3.48(2)
CaF <sub>2</sub> initial (PEBE)					
CaF <sub>2</sub> cub			CaF <sub>2</sub> tetr		
CSR, nm	Period, Å	$\rho$ , g/cm <sup>3</sup>	CSR, nm	Period, Å	$\rho$ , g/cm <sup>3</sup>
45(3)	5.463(3)	3.181(4)	$\approx 14$	$a = 3.734(7)$ $c = 2.875(9)$	3.23(2)

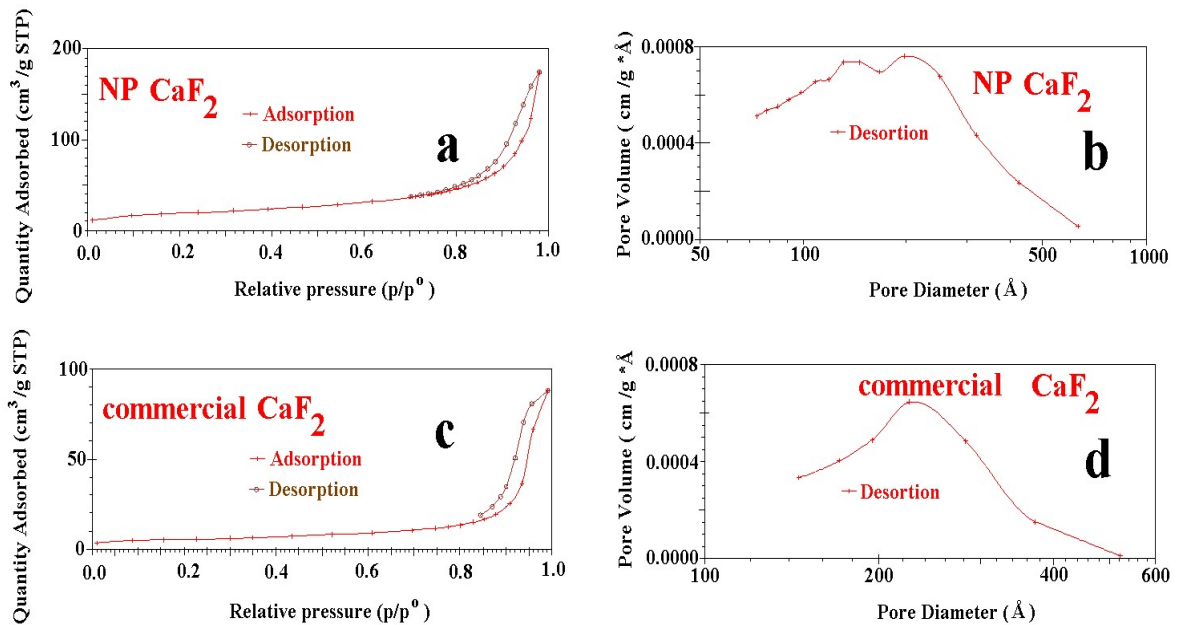


**Fig.1.** Nitrogen adsorption/desorption isotherms (a, c) and pore size distribution curves (b, d) of NP and commercial powder CaF<sub>2</sub>.

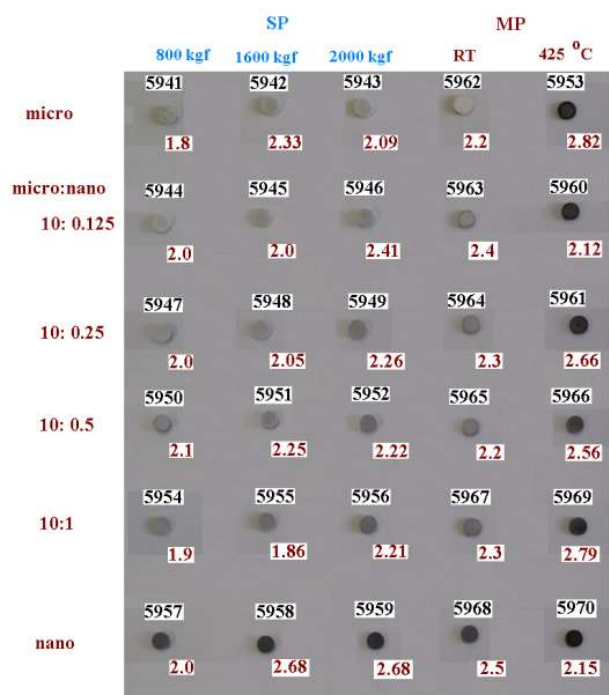


Fig.2. Photos of compacts prepared by the MP and SP methods from the mixes of commercial and synthesized  $\text{CaF}_2$  powders, indicating the density achieved using SP and MP methods.

Both powders are mesoporous powders of type IV (Fig. 1a–1d), with unimodal and multimodal pore size distribution. Table 2 shows the texture properties of the powders. Fig. 2 shows the change in color and density of compacts from the fraction of nanodopant.

Table 2. Textural properties of components of commercial powder and  $\text{CaF}_2$  nanopowder mixtures

Composition	Powder	SSA, $\text{m}^2/\text{g}$	Total pore volume, $\text{cm}^3/\text{g}$	Average pore diameter, (nm)
$\text{CaF}_2$	Commercial	18.5	0.13	25
$\text{CaF}_2$	NP	64.3	0.25	21

In Table 3. are given density of compacts from mixtures of micro and nano  $\text{CaF}_2$  powders and parameters of pressing by MP and SP methods.

Table 3. Density of  $\text{CaF}_2$  compacts and parameters of their pressing by SP and MP methods

Share of NP	SP						MP			
	$P_p$ , 800 kgf	$\rho$ , $\text{g}/\text{cm}^3$	$P_p$ , 1600 kgf	$\rho$ , $\text{g}/\text{cm}^3$	$P_p$ , 2000 kgf	$\rho$ , $\text{g}/\text{cm}^3$	$T_p$ , RT	$\rho$ , $\text{g}/\text{cm}^3$	$T_p$ , 425 °C	$\rho$ , $\text{g}/\text{cm}^3$
0	5941	1.8	5942	2.33	5943	2.09	5962	2.26	5953	2.82
1.25	5944	2.08	5945	2.00	5946	2.41	5963	2.45	5960	2.12
2.5	5947	2.05	5948	2.05	5949	2.26	5964	2.30	5961	2.66
5.0	5950	2.12	5951	2.25	5952	2.22	5965	2.28	5966	2.56
10.0	5954	1.99	5955	1.86	5956	2.21	5967	2.31	5969	2.79
100	5957	2.04	5958	2.68	5959	2.68	5968	2.57	5970	2.15

RT – room temperature,  $P_p$  and  $T_p$  – pressure and pressures temperature,  $\rho$  – compacts density

The total pore volume in NP (Table 2) is twice that of micron powder. High pore volume negatively affects the density of NPs compacts [1], however, SP achieved a higher density of NP compacts (5957–5959, Table 3) over the entire pressure range compared to the density of micron powder compacts (5941–5943, Table 3). The density of NP compacts was influenced by the presence of metal NPls Ca in them, which contributed to a decrease in interparticle friction. Pre-

annealing the original NP in air at 400 °C for 30 minutes significantly affected the density of pure NP compacts (see Table 4).

**Table 4.** Density of CaF<sub>2</sub> compacts, produced from annealed at 400 °C NP CaF<sub>2</sub> and parameters of their pressing by SP and MP methods

Share of NP	SP		MP			
	$P_p$ , 1600 kgf	$\rho$ , g/cm <sup>3</sup>	$T_p$ , 425 °C	$\rho$ , g/cm <sup>3</sup>	$T_p$ , RT	$\rho$ , g/cm <sup>3</sup>
100	5663	2.54	5965	2.84	5670	2.39

Annealing resulted in an increase in the density of a compact from pure NP compressed at 425 °C. The density increased from 2.15 (5970) to 2.84 g/cm<sup>3</sup> (5665) and became comparable to the density of the micron powder compact CaF<sub>2</sub> (5953,  $\rho$  = 2.82 g/cm<sup>3</sup>). However, the density of compacts compressed at RT (5663 and 5670) turned out to be slightly less than the density of compacts from not annealed NP by MP (RT) (2.39 g/cm<sup>3</sup> (5670, Table 4) and 2.57 g/cm<sup>3</sup> (5968, Table 3)) and SP at a pressure of 1600 kgf (2.54 g/cm<sup>3</sup>). This reduction in density further indicates that the presence of metallic NPles Ca in the original NP had a dominant effect on the density of NP compacts. Vacuum sintering at 1000 °C (15 min) of all samples from Table 3 showed that high density matte ceramics were produced from these samples. PCL spectra compacts of pure micro and nano powders and mixtures thereof, recorded at room temperature, in the visible range, are shown on Fig.3.

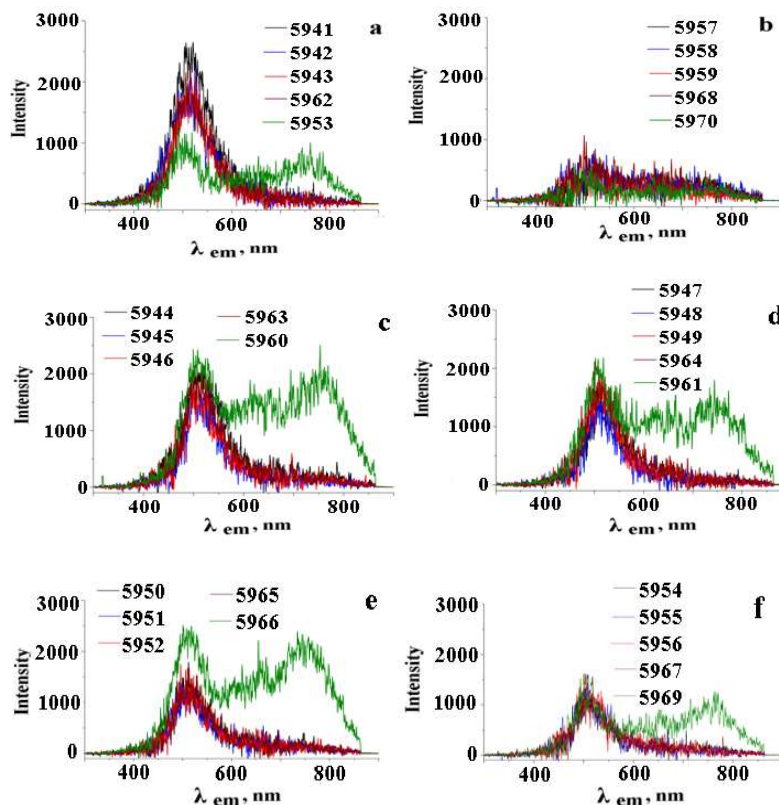


Fig.3. PCL spectra of compact specimens: 5941–5943, 5962, 5963 (a); 595–5959, 5968, 5970 (b); 5944–946, 5963, 5960 (c); 5947–5949, 5964, 5961 (d); 5950–5952, 5965, 5966 (e); 5954–5956, 5967, 5969 (f) in the visible wavelength range.

PCL compact spectra were recorded separately in UV and Vis regions of the spectrum. All spectra (except PCL spectra samples produced by MP at 425 °C) were two broad bands with

maxima at ~315 and 500 nm. The band in the UV region of the spectrum is associated with structural defects such as F centre, H centre, I centre, anion vacancy and/or  $V_k$  centre ( $F^{2-}$  molecular ion), the band in the Vis region of the spectrum – with point defects associated with the  $Mn^{2+}$  doping material in the nodes of the  $CaF_2$  cation lattice [4]. The  $P_p$  and  $T_p$  compressions did not affect the location of the maxima and the shape of the PCL spectra in the UV region of the spectrum, so we excluded these spectra from consideration. Intensity of PCL spectra in Vis region of micron powder compacts  $CaF_2$  (5941–5943, Fig.3a) with an increase in  $P_p$  monotonously decreased. The spectra of samples 5941–5943 and 5962 contained one wide peak (~350–700 nm), and the spectrum arr. 5353 (MP,  $T_p = 4250$  °C) contained three broad peaks at ~500, 650 and 700 nm. The PCL spectra of all NP-spiked compacts (MP,  $T_p = 425$  °C) also contained three peaks each with maxima at ~500, 650 and 700 nm. Accordingly, the PCL spectra of all samples compressed at RT contained only one broad peak with a maximum at 500 nm. On Fig.3b shows PCL compact spectra from pure NP  $CaF_2$  (MP and SP). It can be seen that the samples were practically not luminesized. The weak cathodoluminescence intensity of compacts 5957–5959, 5968 and 5970 is caused by the high concentration of metallic NPles calcium in NP. PCL spectra of compacts from mixtures of micro and nano powders are shown in Fig.3c–3f. The evolution of spectra with increasing concentration of nanoaddition in samples showed the following: (a) monotonous decrease in PCL intensity of samples manufactured by SP and MP methods at RT with increasing proportion of NP additive in mechanical mixtures (Fig.3e–3f); (b)  $T_p$ -main factor that influenced the morphology of PCL spectra of all luminescent samples. Heating the compacts to a temperature of 425 °C resulted in the appearance of a long wave arm in the PCL spectra of micron  $CaF_2$  powder (ref. No. 5963) and samples from powder mixtures (5960, 5961, 5966 and 5961), which contained two wide, overlapping bands in the red (~630 nm) and near infrared ranges ((NIR) (~750 nm). Probably, as a result of the effect of temperature on compacts, vacancies occurred in the fluoride lattice  $CaF_2$  as a result of the removal of fluorine atoms from the surface layers. The appearance of NIR peaks in MP samples at 425 °C is solely due to the addition of NP  $CaF_2$ . In compacts (5663, 5665 and 5670, Table 4) of annealed NP  $CaF_2$  at 400 °C, the dominant peak was also in the red region of the spectrum (599–611 nm), but there was no third peak in the NIR region. This fact shows that pre-annealing of NP  $CaF_2$  at 300–400 °C eliminates most of the defects in the original NP  $CaF_2$ . Consequently, it is possible to produce compacts of higher density from the annealed starting NP than from the annealed NP. Using the MP method to heat the compact to 425 °C, PCL spectra has an intense (up to 50% of the dominant peak intensity) NIR peak that can be controlled by simple thermal annealing of the compact in air. By pre-annealing the nano-additive  $CaF_2$ , it is possible to remove the NIR peak in compacts from pure NP, produced by any methods, and bring the density of the compact using the MP method at 425 °C (5665, Table 4) to the level of 89% of the theoretical density. Smoothed PL spectra of 30 samples are shown on Fig.4.

The PL spectra of micron powder compacts (5941–5943, 5962, 5953) contained two red bands each with maxima at (609–61) and (645–47) nm, regardless of the pressing method. The intensity of PL decreased monotonously (5941–5943) as  $P_p$  increased (SP at RT). Sample 5953 (MP at 425 °C) showed an increase in the intensity of both PL bands, which could be caused by an increase in crystal size at 425 °C. Compacts of pure NP (5957–5959) showed a sharper decrease in PL intensity with an increase in  $P_p$  (SP). Compacts 5968 and 5970 compressed by MP showed the opposite tendency of decreasing intensity with increasing  $T_p$ , which can be explained by the influence of metal Ca particles contained in NP  $CaF_2$ . The type of spectra in samples with a small fraction of nano-additive (1.25) was preserved, as well as in compacts made of micron powder.

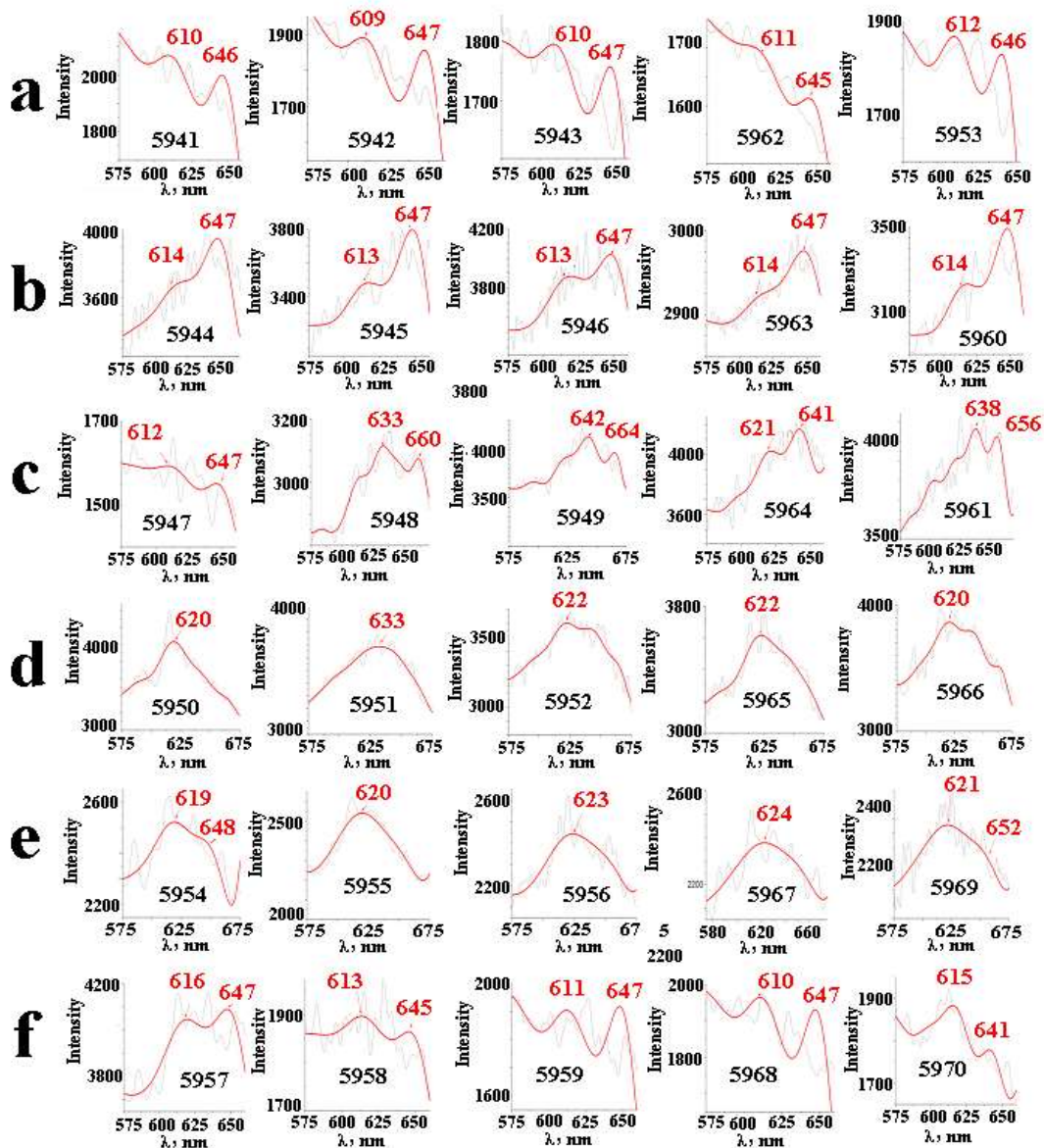


Fig.4. PL spectra of compact specimens: 5941–5943, 5962, 5963 (a); 5944–5946, 5963, 5960 (b); 5947–5949, 5964, 5961 (c); 5950–5952, 5965, 5966 (d); 5954–5956, 5967, 5969 (e); 5957–5959, 5968, 5970 (f) in the visible wavelength range. PL spectra of compacts 5663, 5663 and 5670.

With an increase in the share of nano-additives in compacts, the spectra changed very much. With a fraction of nano-additive 2.5, a third red band appeared in the spectra of individual samples (5948, 5949-SP and 5961-MP at 425 °C) in the 656–664 nm wavelength range, which appears to be associated with the formation of a new F-center in the samples (like all other bands). The high intensity of PL with peaks at 621–638 nm and 656–664 nm was shown by all samples with a nano-additive concentration of 2.5 compared to sample 5947, in which the third band was clearly absent. With an increase in the share of nano-additive to 5–10, regardless of the pressing method, the type of spectra changed towards smoothing of peaks and was observed a gradual transformation of the shape of the spectra into a wide band with one maximum at approximately 619–624 nm. The spectra of individual samples (5952, 5966, 5954 and 5969) showed peaks with maxima at ~ 640 and 660 nm. The peak intensities of compacts with nano-additive fractions of 5–10 with an increase in  $P_p$  at SP decreased monotonously, which indirectly indicated a decrease in the number of defects in

the compacts. With MP compacts with an increase in the proportion of nano-additive from 5 to 10, there was a significant decrease in the intensity of PL, regardless of  $T_p$ . Samples 5946 and 5949, compressed at a pressure of 2000 kgf with minimal proportions of nano-additive (1.25–2.5), had the highest intensity. The maximum intensity was also shown by samples 5964 and 5961 made by the MP method with a nano-additive fraction of 2.5, which makes it possible to consider the above fraction as optimal. Interestingly, the appearance of a blue peak (434 nm) in the PL spectra of compacts (5663 and 5665) compressed from NP CaF<sub>2</sub> annealed at 400 °C (Fig.5). The appearance of a blue peak is associated with an impurity oxygen vacancy [7, 8].

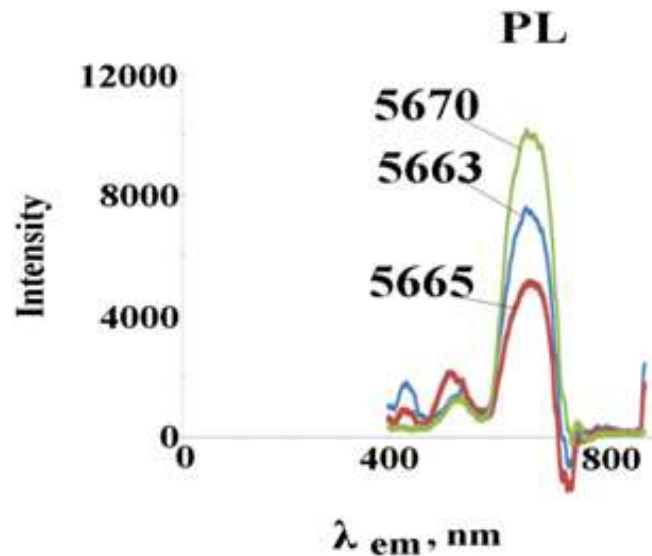


Fig.5. PCL spectra compacts 5663, 5663 and 5670 in Vis spectral region.

#### 4. Conclusion

Compacts of CaF<sub>2</sub> from mixtures of micro and nano powders are made by SP and MP methods. The phase composition, defective structure and concentration of the nanodopant, as well as  $T_p$ , had a major effect on compact density. The density of compacts of pure nano and micro powders reached 84% and 89% of the theoretical density, respectively. Preliminary annealing of NP at 400 °C yielded a compact with a density of 89%. The density of compacts from mixtures did not exceed 76%, however, MP at 425 °C allowed to achieve a density of 88%. There is shown the correlation between properties of nano-additive (oxygen vacancies, concentration of NPles Ca in initial NP) and cathode-photoluminescent spectra of compacts. A blue peak was found in the PL spectra of annealed NP compacts. Sintering of compacts at 1000 °C in vacuum resulted in the formation of dense (90–99%) matte ceramics of CaF<sub>2</sub>, promising for use as solid-state luminescent dosimeters.

#### Acknowledgement

This work was supported by the Russian Science Foundation, project no. 22-19-00239.

#### 5. References

- [1] Kuznetsov S.V., Alexandrov A.A., Fedorov P.P., *Inorg. Mater.*, **57**, 555, 2021; doi: 10.1134/S0020168521060078
- [2] Sokovnin S.Yu., Ilves V.G., *Ferroelectrics*, **436**, 101, 2012; doi: 10.1080/10584587.2012.730951

- [3] Ilves V.G., et al., *Phys. Sol. State.*, **61**, 2200, 2019; doi: 10.1134/S1063783419110179
- [4] Ilves V.G., Sokovnin S.Yu., Zuev M.G., Murzakaev A.M., *J. Magn. Magn. Mater.*, **504**, 166666, 2020; doi: 10.1016/j.jmmm.2020.166666
- [5] Ilves V.G., Sokovnin S.Yu., Uimin M.A., *J. Fluor. Chem.*, **253**, 109921, 2022; doi: 10.1016/j.jfluchem.2021.109921
- [6] Rodríguez R., Correcher V., Gómez-Ros J.M., Plaza J.L., Garcia-Guinea J., *Radiat. Phys. Chemistr.*, **188**, 109621, 2021; doi: 10.1016/j.radphyschem.2021.109621
- [7] Wang P., et al., *J. Eu. Ceram. Soc.*, **41**, 4609, 2021; doi: 10.1016/j.jeurceramsoc.2021.03.014
- [8] Wang P., et al., *J. Eur. Ceram. Soc.*, **42**, 245, 2022; doi: 10.1016/j.jeurceramsoc.2021.10.004